ORIGINAL PAPER

Deterministic seismic hazard assessment for Sultanate of Oman

A. Deif · I. El-Hussain · K. Al-Jabri · N. Toksoz ·
S. El-Hady · S. Al-Hashmi · K. Al-Toubi · Y. Al-Shijbi ·
M. Al-Saifi

Abstract The Sultanate of Oman forms the southeastern part of the Arabian plate, which is surrounded by relatively high active tectonic zones. Studies of seismic risk assessment in Oman have been an important on-going socioeconomic concern. Using the results of the seismic hazard assessment to improve building design and construction is an effective way to reduce the seismic risk. In the current study, seismic hazard assessment for the Sultanate of Oman is performed through the deterministic approach with particular attention on the uncertainty analysis applying a recently developed method. The input data set contains a defined seismotectonic model consisting of 26 seismic zones, maximum magnitudes, and 6 alternative ground motion prediction equations that were used in four different tectonic environments: obduction zone earthquake (Zagros fold thrust belt), subduction zone earthquakes (Makran subduction zones), normal and strike-slip transform earthquakes (Owen and Gulf of Aden zones), and stable craton seismicity (Arabian stable craton). This input data set

yielded a total of 76 scenarios at each point of interest. A 10 % probability that any of the 76 scenarios may exceed the largest median ground acceleration is selected. The deterministic seismic hazards in terms of PGA, 5 % damped spectral acceleration at 0.1, 0.2, 1.0 and 2.0 s are performed at 254 selected points. The ground motion was calculated at the 50th and 84th percentile levels for selected probability of exceeding the median value. The largest ground motion in the Sultanate of Oman is observed in the northeastern part of the country.
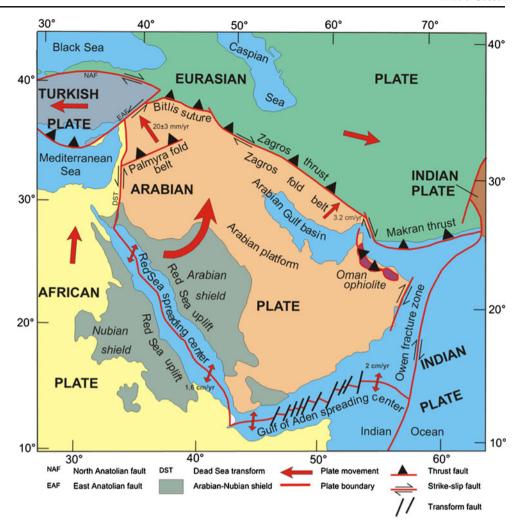
Introduction

The Sultanate of Oman occupies the southeastern corner of the Arabian plate with proximity to four main active tectonic margins. Active tectonics of this region is dominated by the collision of the Arabian plate with the Eurasian plate along the Zagros and Bitlis thrust systems, subduction of the Arabian plate beneath the Eurasian plate along the Makran subduction zone, the transformation of Owen fracture zone that separates the Arabian and the Indian plates, and rifting and seafloor spreading in the Gulf of Aden (Fig. 1). With the exception of the Oman Mountains' range, which shows evidence for recent deformation (Johnson 1998; Kusky et al. 2005), the major part of the tectonic action on Oman is remote and takes places along the prementioned four margins as revealed by the observed high rate of the seismic activity (Fig. 2).

The seismicity data shown in Fig. 2 is taken from the catalogue of El-Hussain et al. (2012). The initial catalogue was compiled for a spatial region spanning from 42° to 66° E and 10° to 32° N and included all events having an assigned magnitude of 3.0 and above on any magnitude scale. They used information from several international,

A. Deif · I. El-Hussain (✉) · S. Al-Hashmi · K. Al-Toubi ·
Y. Al-Shijbi · M. Al-Saifi
Earthquake Monitoring Center, Sultan Qaboos University,
Muscat, Oman
e-mail: elhussain@squ.edu.om

K. Al-Jabri
Department of Civil and Architectural Engineering,
Sultan Qaboos University, Muscat, Oman

N. Toksoz
Massachusetts Institute of Technology, 77 Massachusetts Avenue,
Cambridge, MA 02139, USA

A. Deif · S. El-Hady
National Research Institute of Astronomy and Geophysics,
Helwan, Egypt

S. El-Hady
Faculty of Earth Science, Geophysics Department,
King Abdulaziz University, Jeddah, Saudi Arabia

Fig. 1 Major tectonic elements surrounding the Arabian plate (Johnson 1998)

regional, and local databases to compile one comprehensive catalogue. In addition, many individual studies on specific events or region were also consulted to gather additional information regarding earthquakes of considerable size. They removed all duplications and applied a proper priority scheme to select the best earthquake parameters from the available catalogues. To ensure catalogue magnitude homogeneity, El-Hussain et al. (2012) converted all events for which moment magnitudes were not reported into this scale.
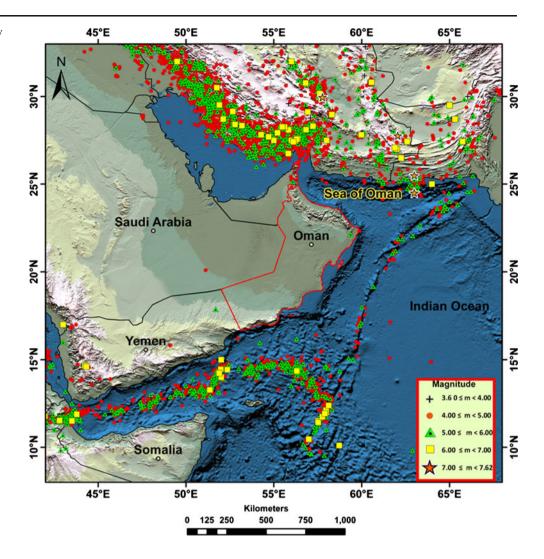
The number of large earthquakes documented in the Arabian Peninsula is very low. The seismotectonic settings around Oman strongly suggest that large earthquakes are possible, particularly along the Arabian plate boundaries. Large earthquakes in these surrounding zones can significantly produce damaging effect to structures in Oman. Low-frequency components of the generated seismic waves can travel very far with very long duration and without much attenuation. These are the most critical waves of the remote sources because they can cause resonant vibrations in structures with low natural frequencies.

The most effective way to reduce disasters caused by earthquakes is to estimate the seismic hazard and to disseminate this information for use in improved building design and construction. Seismic hazard estimates, however, are not available for Oman. Therefore, it is crucial to fill this critical gap and to increase the ability of the country to assess the level of seismic hazard. The seismic activity in and around Oman, emphasized the importance of defining the seismic zoning of the country and the need for the assessment of seismic hazard based on the available geophysical, geological, and seismological database.

Seismic hazard could be assessed using a probabilistic seismic hazard assessment (PSHA) or deterministic seismic hazard assessment (DSHA) approaches. The PSHA advocates that the likelihood of occurrence is considered in view of the fact that the life of a structure is very short compared to the recurrence intervals of large events. The DSHA proposes a design for the "maximum earthquake", that is the one that will produce the most severe ground motion at the site. Both of these analyses require a comprehensive database on seismicity, tectonics, geology, and attenuation characteristics of the seismic waves in the area of the structure. For engineering dynamic analysis, the ground motion time history is required. The ground motion time histories can be

Fig. 2 Instrumental seismicity of Oman and its surrounding in terms of moment magnitude in the period from 1904 to 2008

derived from PSHA or DSHA. However, the time histories derived from PSHA do not associate with any individual, but many earthquakes. This is one of the disadvantages of PSHA. On the other hand, it is straightforward for DSHA to provide time histories because DSHA determines earthquakes that have the most significant impacts. In this study, the DSHA approach is carried out to evaluate the seismic hazard.

The conventional deterministic seismic hazard approach defines the seismic source or sources that might affect the site of interest and then estimates the maximum possible earthquake magnitude for each of these sources. By assuming each of these maximum earthquakes to occur at a location that places the earthquake at the minimum possible distance to the site, the ground motion is predicted, mostly, utilizing an empirical attenuation relation.

The deterministic approach is subject to the epistemic uncertainties (Abrahamson 2000; Stepp et al. 2001). In the current study, the epistemic uncertainties are treated by taking alternatives for the ground motion prediction equations, which in turn implicate several different estimates of

the ground motion. The deterministic approach suffers also from the aleatory uncertainties in various input parameters used to describe the seismicity and the ground motion prediction equation. The aleatory variability in ground motion models is usually treated in a very simple manner in conventional deterministic approach, whereby the median or 84th percentile level of motion from the selected ground motion model is calculated for the magnitude–distance combination of the design earthquake scenario. A weakness in this DSHA practice is that it provides no mechanism for dealing with the possibility of larger ground motions.

In this study, the deterministic hazard and its associated uncertainty for the Sultanate of Oman is assessed using the method proposed by Campbell (2005) and applied by Deif et al. (2009). This method of calculation treats the uncertainty problem and provides a chance to provide different percentile levels at different desired probability levels of exceeding the largest median ground motion. Thus, the chance of exceeding the design ground motion is addressed directly. This provides great flexibility to the engineer to

select the proper level of conservatism according to the importance of his project.

Methodology

The outline of the procedure developed by Campbell (2005) for the deterministic seismic hazard assessment is as follows:

1. Delineation of the seismic sources of possible impact on the Sultanate of Oman
2. Assessment of the maximum earthquake of each seismic source.
3. Select a set of earthquake scenarios (M, R). Scenario means earthquake of specific magnitude (M) at specific distance (R) from the site of interest.
4. Calculate the median ground motion for each scenario (y' |m,r)
5. Define the largest median value among y' (y_{max})
6. Select desired exceedance probability of y_{max}:
$P [Y > y_{max} |m,r]$
7. Calculate fractile (percentile) of y_{max}:

$$x = -P[Y > y_{max}|m,r] \qquad (1)$$

8. Determine standard normal variate of x (Z_x)
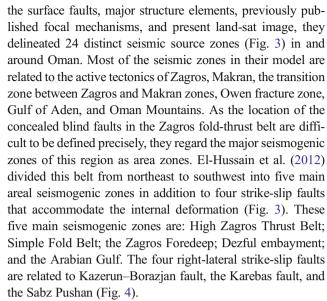9. Compute at the site of interest the xth percentile value of y_{max}:

$$\log y_{max,x} = \log y_{max} + Z_x \, \sigma_{\log Y}^a \qquad (2)$$

The only difference between the current deterministic seismic hazard approach and the conventional one is the use of the logic tree to capture uncertainty. The logic tree is the same as that used for PSHA to capture epistemic uncertainty, except that the weights assigned to each branch, and thus to the entire path through the logic tree, are applied to the logarithm of the ground motion rather than to the exeedance frequency of the ground motion. Details about the treatment of such uncertainty could be found in Thenhaus and Campbell (2003).

Definition of seismic sources of possible impact on the Sultanate of Oman

The definition of seismogenic sources involves the identification of earthquake generating faults and their preferred location (Reiter 1991). In regions with difficult fault identification, the seismotectonic sources are identified as areas of grouped seismicity in which the earthquake activity and stress field orientation are assumed to be relatively uniform in terms of type and distribution of earthquakes.

In the current study, we used mainly the seismotectonic model developed by El-Hussain et al. (2012) to describe the geographical distribution of earthquake source zones that might affect Oman. Based upon the compilation of seismicity,

the surface faults, major structure elements, previously published focal mechanisms, and present land-sat image, they delineated 24 distinct seismic source zones (Fig. 3) in and around Oman. Most of the seismic zones in their model are related to the active tectonics of Zagros, Makran, the transition zone between Zagros and Makran zones, Owen fracture zone, Gulf of Aden, and Oman Mountains. As the location of the concealed blind faults in the Zagros fold-thrust belt are difficult to be defined precisely, they regard the major seismogenic zones of this region as area zones. El-Hussain et al. (2012) divided this belt from northeast to southwest into five main areal seismogenic zones in addition to four strike-slip faults that accommodate the internal deformation (Fig. 3). These five main seismogenic zones are: High Zagros Thrust Belt; Simple Fold Belt; the Zagros Foredeep; Dezful embayment; and the Arabian Gulf. The four right-lateral strike-slip faults are related to Kazerun–Borazjan fault, the Karebas fault, and the Sabz Pushan (Fig. 4).

Makran zone is divided into west and east Makran, based upon the dramatic change in the seismicity pattern in these two sections. The Owen Fracture zone is divided into the Owen and Murray seismic zones due to the change in the fracture trend. The seismicity in the Gulf of Aden is modeled by three main seismogenic zones, Western and Eastern Gulf of Aden, which are separated by the Alula Fartaq transform fault (Zone No 3). Seismicity level decreases drastically from the central axis of the Gulf of Aden and thus the seismicity cannot be stationary from the space and time point of view. Therefore, the Northeastern Gulf of Aden (Zone No. 4) was selected to represent this lower seismicity level towards the northeastern part of the Gulf of Aden. Yemen zone is included because the 1982 event in Yemen was felt in southern Oman.
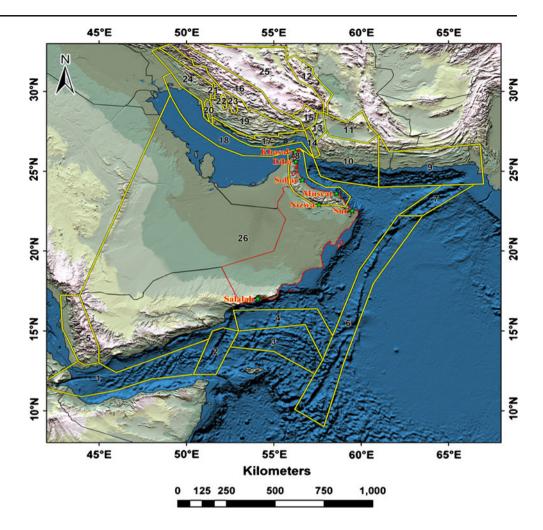
In addition to the 24 distinct seismic sources, two background seismicity zones were selected to model the floating earthquakes that are located around the studied area. The Iranian background zone includes the central Iran area between the Main Zagros Thrust Fault and the Gowk Fault. The Arabian background zone extends to include part of the Arabian Peninsula and the western part of the Arabian Sea (Table 1).

Definition of maximum earthquake for each seismic source

Following the definition of seismotectonic sources, the next step in the seismic hazard analysis is the definition of the maximum earthquake (max M) for each of the identified seismotectonic sources. Selection of the maximum earthquake (M_{max}) has a considerable impact on the hazard results. M_{max} is possibly the most difficult parameter to assess in the study area because the database in many seismogenic zones is statistically very limited. Therefore, the maximum magnitudes are determined with varying methods depending on the nature the source zone (fault or

Fig. 3 The seismotectonic source model for the area of study, the locations of major cities in Oman are also shown

area source) and robustness of the available seismological database of each zone.

Regression relationships between earthquake magnitude and fault parameters have been developed during the past several decades (e.g., Slemmons 1977; Bonilla et al. 1984; Wells and Coppersmith 1994; Hanks and Bakun 2002). Both geological and historical observations of the rupture history of highly active and carefully investigated faults indicate that faults do not rupture their entire length in a single event, except in unusual structural situations (Allen 1975). A conservative practice is to assume a fraction up to one half the total length of a fault to rupture in a single event. Along the San Andreas Fault system, this fraction is one third to two fifths (Reiter 1991). Slemmons (1982) showed that this fraction of the fault length decreases as the fault length itself decreases. His study showed rupture lengths range from about 17 to 33 % of the total fault lengths, with the smaller value typical of faults less than about 200 km long and the larger value typical of faults having lengths of more than 1,000 km.

With the exception of Gowk fault with a length of about 450 km, all the fault sources in the current study have lengths less than 200 km. Twenty percent of the total fault

length is selected to represent a conservative fractional length to apply to the studied faults, where 40 % of Gowk fault length is supposed to rupture in a single earthquake. The empirical relationships of Wells and Coppersmith (1994) are used to calculate the maximum magnitude for the fault sources when consistent data about the total length and fault type are available (Table 2).
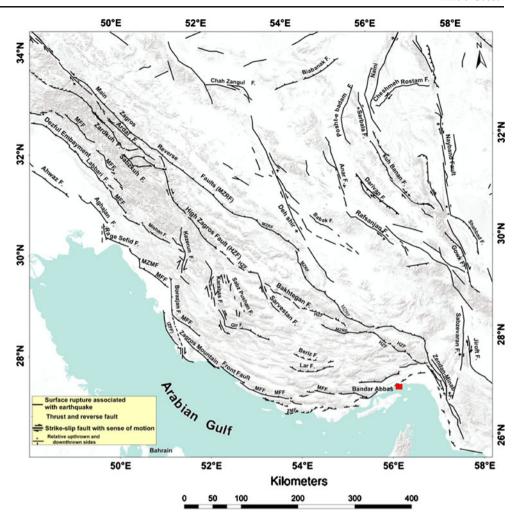
For the remaining area seismic zones with sufficient seismological information, the maximum magnitude was estimated using the statistical procedure of Kijko (2004), using the following equations:

$$m_{\max} = m_{\max}^{\mathrm{obs}} + \int_{m_{\min}}^{m_{\max}} [F_m(m)]^n \, dm \qquad (3)$$

where $F_m(m)$ is the cumulative density function (CDF) of magnitude. From this equation, an estimated value of $m_{\max}$ can be obtained only by iteration. This equation states that $m_{\max}$ is equal to the largest observed magnitude $(m_{\max}^{\mathrm{obs}})$ plus an amount $= \int_{m_{\min}}^{m_{\max}} [F_m(m)]^n$. This equation is valid for any CDF, $F_m(m)$, and does not require the fulfillment of any additional conditions. It may also be used when the exact number of earthquakes, n, is not known. In this case, the

Fig. 4 The main fault zones of Zagros thrust belts (modified after Hessami et al. 2003)

number of earthquakes can be replaced by λT. Such a replacement is equivalent to the assumption that the number of earthquakes occurring in unit time conforms to a Poisson distribution with parameter λ, with T the span of the seismic catalogue. It is also important to note that since the value of the integral Δ is never negative, the equation provides a value of m_{max}, which is never less than the largest magnitude already observed. The integration Δ for the Gutenberg–Richter relation, that bounded from above is given by:

$$\Delta = \int_{m_{min}}^{m_{max}} \left[\frac{1 - \exp[-\beta(m - m_{min}]}{1 - \exp\left[-\beta\left(m_{max}^{obs} - m_{min}\right)\right]} \right]^n dm \qquad (4)$$

This integral is not simple to evaluate, therefore Kijko (2004) replaced $[F_m(m)]^n$ by its Cramer (1961) approximation $\exp\{-n[1-[F_m(m)]]\}$. Then, the integral is solved to result in m_{max}.

In the Oman Mountains and the Arabian background seismic sources, the maximum magnitude was obtained by adding 0.5 units to the maximum observed magnitude (Table 2).

Ground motion estimation

For each calculated maximum magnitude value, the associated strong-motion parameter (acceleration) at each site of interest should be estimated using an empirical attenuation relationship. Usually, the assumption is made that the maximum earthquake occurs at a location in the source closest to the site of interest. For the magnitude and distance ranges currently well covered universally by data, ground motion amplitudes deviation from logarithmic mean predicted by attenuation models are common (e.g., Abrahamson 2000; Bommer et al. 2004). Thus, uncertainties in ground motion prediction models could be large and an essential component of seismic hazard assessment is to identify and quantify them to the extent possible.

Accounting for ground motion variability is not a conservatism that can be included or excluded based on engineering judgment, but hazard studies that exclude this variability are simply wrong (Abrahamson 2006). The standard deviation of the ground motion from the modeled values is used to account for the variability of ground motion.

Table 1 Seismic sources of seismotectonic source model for the PSHA

No.	Source name
1	Western Gulf of Aden
2	Alula Fartaq Zone
3	Eastern Gulf of Aden
4	Northeastern Gulf of Aden
5	Yemen
6	Owen
7	Murray Zone
8	Oman Mountains
9	East Makran
10	West Makran
11	Jaz Murian Depression
12	Gowk Fault
13	Jiroft–Sabzevaran Fault
14	Minab–Zendan Fault
15	Aliabad
16	High Zagros Zone
17	Zagros Foredeep
18	Arabian Gulf
19	Zagros Simple Fold
20	Borazjan Fault
21	Kazerun Fault
22	Karebas Faults
23	Sabz Pushan Fault
24	Dezful Embayment
25	Iranian Background Zone
26	Arabian Background Zone

Table 2 Recurrence parameters using doubly bounded exponential seismicity model

Zone	Zone name	M_{max}	σM_{max}	M_{max} (obs)
1	Western Aden	6.9	0.32	6.8
2	Alula Fartaq	6.7	0.38	6.5
3	Eastern Aden	6.5	0.23	6
4	NE Aden	5.8	0.3	5.8
5	Yemen	6.6	0.33	6.4
6	Owen	6.9	0.36	6.7
7	Murray	6.4	0.68	5.8
8	Oman Mnt.	6.0[a]	0.5	5.5
9	East Makran	8.2	0.21	8.1
10	West Makran	7.8	0.23	7.7
11	Jaz Murian	7.1	0.31	7
12	Gowk Fault	7.8[b]	0.52	7.1
13	Jiroft–Sabzevaran Fault	6.8[b]	0.25	5.8
14	Minab–Zendan	6.7[b]	0.31	5.8
15	Aliabad	7.1	0.52	6.6
16	High Zagros Thrust	6.8	0.3	6.7
17	Zagros Foredeep	6.9	0.31	6.8
18	Arabian Gulf	6.1	0.14	6.0
19	Zagros Simple Fold	7.2	0.31	7.1
20	Borazjan Fault	6.8[b]	0.42	5.5
21	Kaserun Fault	6.5[b]	0.57	5.9
22	Karebas Fault	6.5[b]	0.32	4.6
23	Sabz Pushan Fault	6.4[b]	0.41	6.1
24	Dezful Embayment	6.0	0.34	5.8
25	Iranian Background	6.7	0.27	6.7
26	Arabian Background	5.7[a]	0.5	5.2

[a] Maximum observed magnitude plus 0.5; when not specified, maximum magnitude is calculated using Kijko (2004)

[b] Maximum magnitude is calculated using the empirical relationships of Wells and Coppersmith (1994)

The scarcity and lack of ground motion acceleration records in the Sultanate of Oman makes it a must to apply already-developed ground motion scaling relationships. Alternative ground motion prediction relationships are selected to predict the seismic hazard within the various considered tectonic environments in order to account for the epistemic uncertainty. This, in turn, implicates several different estimates of the ground motion. Six different ground motion prediction relationships are selected. These relationships have been widely used in the seismic hazard assessment all over the world.

We used the models of Ambraseys et al. (1996), Abrahamson and Silva (1997), and Boore et al. (1997) to model the ground motions of the earthquakes occurring within the active shallow crustal seismogenic zones. The models of Youngs et al. (1997) and Atkinson and Boore (2003) are used to model the ground motions of the Makran subduction zone earthquakes. For the Arabian stable craton earthquakes, the model of Atkinson and Boore (2006) with stress drop of 140 bar is used. The definition of the Arabian

Peninsula as stable craton is not unambiguously confirmed (Aldama Bustos et al. 2009). Thus, the three ground motion scaling relationships of the active shallow seismicity were used in conjunction with Atkinson and Boore (2006) relationships to model the stable craton ground motion. The characteristics of the selected ground motion prediction relationships are shown in Table 3. For the active regions like Zagros, the equation of Ambraseys et al. (1996) is derived from datasets of European and Middle Eastern strong-motion data that include records from Iran. There is increasing evidence that motions in Western North America, where the data of Boore et al. (1997) were taken, are broadly similar to those from this region (e.g., Stafford et al. 2008).

Combining two or more ground motion prediction relationships within hazard calculations requires several conversions to be made, because there are several definitions available for

Table 3 Characteristics of the ground motion scaling relationships

Model	Mag.	M_{min}	M_{max}	Dist.	D_{max}	Horizontal comp.	Faulting mechanism	Tectonic
Ambraseys et al. (1996)	M_S	4.0	7.5	R_{JB}	200	Larger horizontal	Unspecified	Shallow active
Boore et al. (1997)	M_W	5.5	7.5	R_{JB}	80	Random horizontal	S.S/reverse others	Shallow active
Abrahamson and Silva (1997)	M_W	4.4	7.4	R_{rup}	220	Geometric mean	Reverse/reverse-oblique/others	Shallow active
Youngs et al. (1997)	M_W	5.0	8.2	R_{rup}	500	Geometric mean	Interface/in-slab	Subduction zones
Atkinson and Boore (2003)	M_W	5.0	8.3	R_{rup}	550	Random horizontal	Interface/in-slab	Subduction zones
Atkinson and Boore (2006)	M_W	3.5	8.0	R_{rup}	1000	Unspecified	Unspecified	Stable regions

R_{rup} the minimum distance between the rupture and the site, M_{min} and M_{max} are the minimum and maximum magnitude in the model data set, respectively, *S.S* is strike-slip faulting, D_{max} is the maximum distance in the data set

both the predicted ground motion parameters and the explanatory parameters within the ground motion prediction relationships. Therefore, alternative inputs and outputs must be transformed into common metrics (Bommer et al. 2005). All of the models used are expressed in terms of moment magnitude except Ambraseys et al. (1996) (see Table 3). Thus, Ambraseys and Free (1997) relationship was used to transform the ground motion prediction relationships into the moment magnitude scale.

The issue of obtaining compatibility among ground motion prediction equations using different distance metrics has been addressed in detail by Scherbaum et al. (2004), who determined explicit distance conversion relations using regression analysis on simulated data based on well-established scaling laws. The functional forms of these relations are magnitude and distance dependent and are expressed as polynomials with associated distributions. They demonstrated that, for all practical purposes, most popular distance metrics can be related to the Joyner and Boore (1981) distance (R_{JB}) using models based upon gamma distribution to express the shape of the residual function. In the current DSHA analysis, the conversion into R_{JB} is done applying the conversions of Scherbaum et al. (2004).

Ground motion prediction equations have employed a variety of definitions for the horizontal component of motion based on different treatments of the two horizontal traces from each accelerogram. When equations using different horizontal component definitions are combined in a logic tree framework for seismic hazard analysis, adjustments need to be made to both the median values of the predicted ground motion parameter and to the associated aleatory variability to achieve compatibility among the equations. Ground motion scaling relations for which the horizontal component is not defined as geometric mean of the two horizontal components are adjusted into this definition using the relationships of Beyer and Bommer (2006).

Statistical treatment and estimated ground motion values

The deterministic seismic hazards in terms of peak ground acceleration (PGA), 5 % damped spectral acceleration on rock at 0.1, 0.2, 1.0, and 2.0 s are performed at 254 points of interest (Fig. 5). Seismic hazard at these sites comes from the large relatively deep earthquakes occurring on the Makran zone, large earthquakes occurring on the Zagros fold belt and Zagros thrust, moderate seismicity from the Owen–Murray zone, Oman Mountains, and the Arabian background zone. The maximum magnitude of the Oman Mountains and the Arabian background zones were placed at a distance of 15 km from each site inside these two seismogenic zones. The largest value (y_{max}) of the 76 median ground motions at each of the 254 points is selected. A desired exceedance probability of 10 % was selected such that any of the proposed scenarios exceeds these largest median ground motions: $P[Y>y_{max}|m,r]$. The scenarios that obey these probabilities are identified based on the standard deviation given by different authors for their ground motion prediction equations.
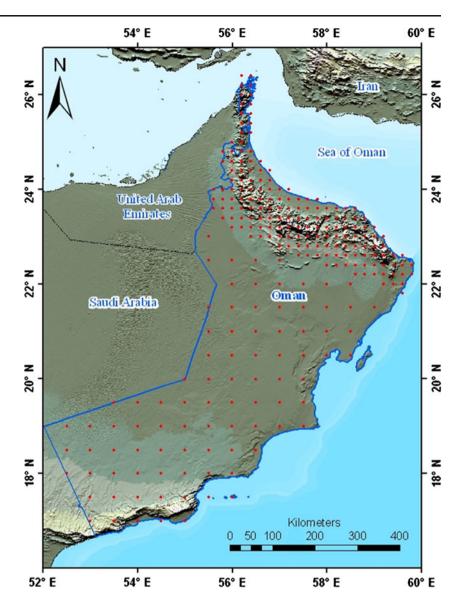
The mean value of the percentiles and their standard deviation from the mean are then calculated and a standard normal variate is determined (Z_x). Finally, the mean and 84th percentile values of the maximum ground motion at rock were computed using Eq. (2).

Seismic hazard maps

The production of seismic hazard maps can be considered as the first step towards taking counter measures against earthquake threat. The aim of such maps is to show the variation in seismic hazard within a region and to provide guidance as to the expected levels of ground motion. The mean and 84th percentile PGA and the 5 % damped horizontal spectral acceleration values at 0.1, 0.2, 1.0, 2.0 s spectral periods were mapped (Figs. 6, 7, 8), so that can be used to generate a spectrum for each node on the hazard maps for the range of periods important for common engineered structures.

Fig. 5 Location of the selected 254 points used for deterministic seismic hazard assessment

Due to their proximity from the points of interest, Oman Mountains and the Arabian background seismogenic sources have the greatest impact on the hazard assessment at most of the interested sites, especially for short spectral period hazards. The DSHA maps delineate the relatively higher seismic hazard regions at the northeastern part of the country from the remaining regions, which is characterized with their relatively lower hazard levels. The mean PGA across Oman ranges from 80 cm/s in the south and middle parts up to about 160 cm/s at the extreme north, and these values becomes slightly higher for the 84th percentile PGA (Figs. 6a, b).

Figure 6c and d show the mean and 84th percentile 5 % damped horizontal spectral acceleration values at 0.1 s spectral period. The maximum ground motion values are associated with the 5 % damped horizontal spectral acceleration with a period of 0.2 s (5 Hz), where the maximum ground motions are 320 and 358 cm/s for mean and 84th percentile

values, respectively at the most northern part of the country (Fig. 7a, b). Compared with countries of high seismic hazard, the hazard in Oman is low in the southern and middle parts of the country, and moderate in the northeastern part. The plots of the hazard maps of 1 and 2 s spectral periods (Figs. 7c, d and 8a, b) are much lower than the ones for higher frequencies.

Discussion

The seismic hazard assessment in Oman presented in the current study was developed with full consideration of the limited database and scientific knowledge regarding the seismogenic nature of the region, particularly the Oman Mountains. Better seismic hazard assessment could be reached if the following three areas of further study are achieved: (1) historical and contemporary earthquake studies, (2) studies in contemporary
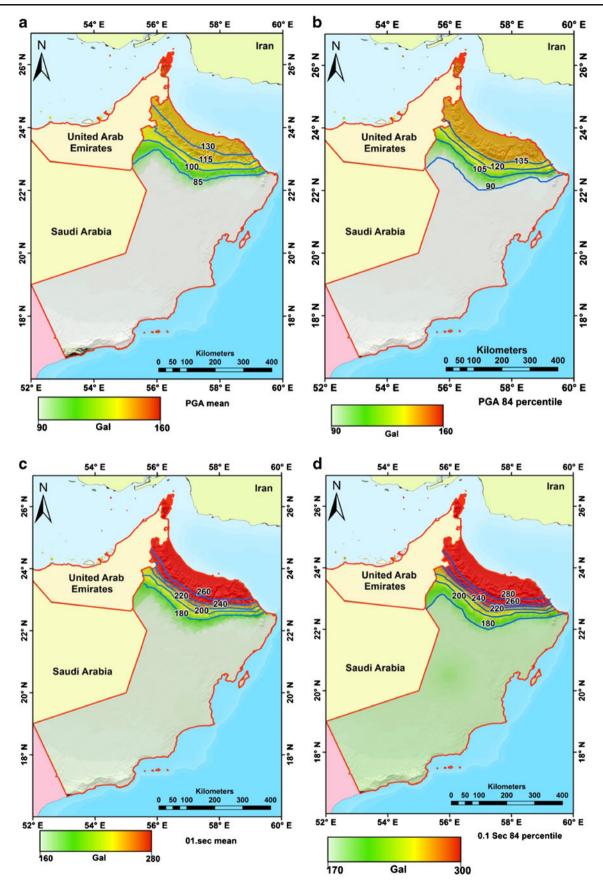
Fig. 6 Mean and 84th percentile peak ground acceleration (**a** and **b**) and mean and 84th percentile damped 5 % spectral acceleration at 0.1 s (**c** and **d**)
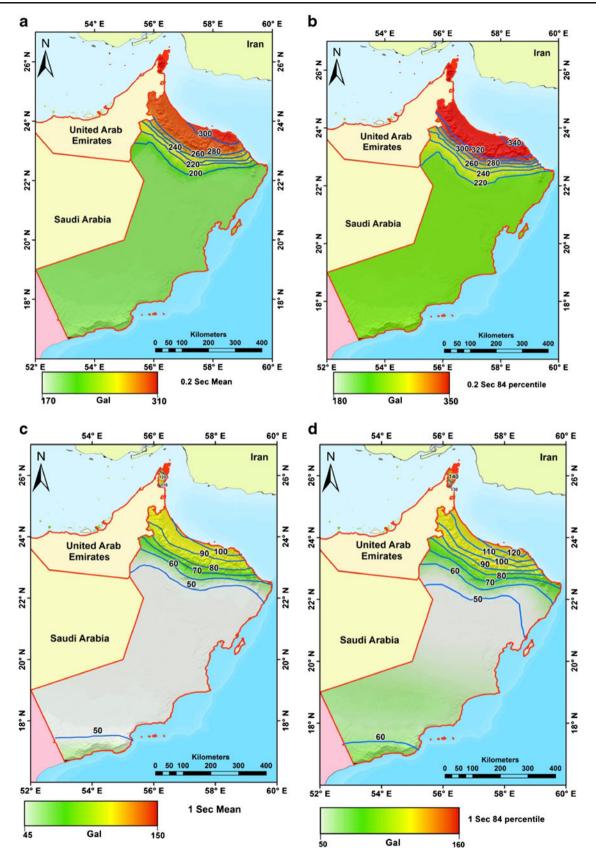
Fig. 7 Mean and 84th percentile damped 5 % spectral acceleration at 0.2 s (**a** and **b**) and mean and 84th percentile damped 5 % spectral acceleration at 1.0 s (**c** and **d**)
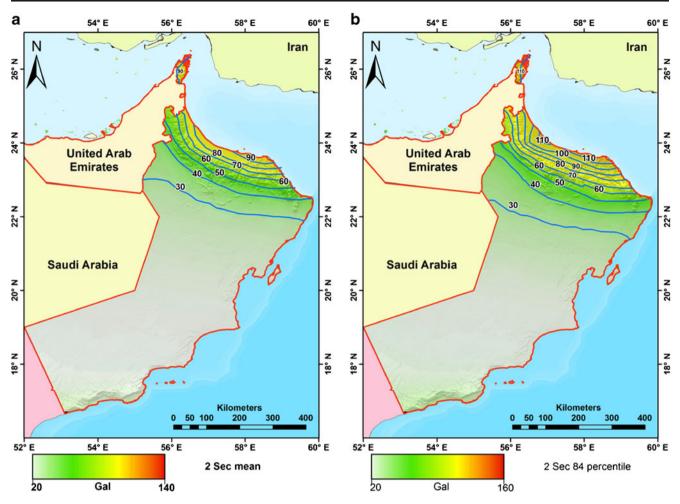
Fig. 8 Mean and 84th percentile spectral acceleration at 2.0 s (**a** and **b**)

tectonics and paleoseismicity in Oman (especially at Oman Mountains), and (3) developing representative regional ground motion scaling relationships for Oman.

Exact knowledge of ground motion prediction relationships is lacking for the area of interest. Therefore, several widely differing and competing alternatives are proposed by different investigators (epistemic uncertainties). As there is no simple way to select the optimum and the most effective alternative, median and 84th percentile values of the strong-motion parameter obtained from several physically plausible models are calculated. The authors believe that the range of the variability was wide enough to result in a conservative unbiased estimate of the seismic hazard.

The problem with the deterministic approach is that the worst-case ground motion will usually be large with a larger cost impact on design, and they are so rare that the high cost is not justified. If there is no large impact on cost or they are not rare, then the worst-case ground motion may be appropriate for design. In the current approach, the mean percentile level with 10 % probability of exceeding the maximum median ground

motion was considered as a reasonable PGA as a "conservative" earthquake magnitude was being used. Each mean value is the maximum of maxima median ground motions at each site. One common view is that using a larger number of standard deviations would be "piling conservatism on top of conservatism" (Abrahamson 2006). This is because the selected earthquakes in Oman Mountains and the Arabian background seismic zones are so rare that the ground motion should not also have to be rare with larger number of standard deviations.

The deterministic seismic hazard maps in the current study deal with ground motion on rock, thus the current analysis did not consider the amplification of soils or basins responses. These factors can change the ground motions and should be considered in the analysis of any site with ground conditions different from rock.

Comparison between the hazard results of the current study and probabilistic one of El-Hussain et al. (2012) indicates that the results of the deterministic seismic hazard assessment for most locations are higher than the probabilistic one even for the higher return period (2,475 years).

This is expected because the deterministic approach proposes design for the worst-case ground motion, which will produce the most severe ground motion at a site. If the probabilistic hazard level at any site is higher than the deterministic one, the hazard level calculated using the deterministic approach (worst case) should be considered.

Conclusion

Seismic hazard assessment in the current study provides a quantitative evaluation of the nature of ground shaking in the Sultanate of Oman that could be induced by future maximum earthquakes. In order to provide the engineers and planners with complete information on which they must base their decisions, the hazard assessment is identified and associated uncertainties are quantified. The final results consist of seismic hazard maps expressed in terms of median ground motion and 84th percentiles for peak ground and spectral acceleration.

References

Abrahamson NA (2000) State of the practice of seismic hazard evaluation. Proc GeoEng 2000 1:659–685, Melbourne, Australia

Abrahamson NA (2006) Seismic hazard assessment: Problems with current practice and future development. First European Conference on Earthquake Engineering and Seismology, Geneva, Switzerland, 3–8 September 2006, 17p.

Abrahamson NA, Silva WJ (1997) Empirical response spectra attenuation relations for shallow crustal earthquakes. Seismol Res Lett 68:94–127

Aldama Bustos G, Bommer JJ, Fenton CH, Staford PJ (2009) probabilistic seismic hazard analysis for rock sites in the cities of Abu Dhbi, Dubai and Ra's Al Khymah, United Arab Emirates. Georisk, 3: 1–29

Allen CR (1975) Geological criteria for evaluating seismicity. Geol Soc Am Bull 86:1041–1075

Ambraseys NN, Free MW (1997) Surface-wave magnitude calibration for European region earthquakes. J Earthq Eng 1:1–22

Ambraseys NN, Simpson KA, Bommer JJ (1996) The prediction of horizontal reponse spectra in Europe. Earthquake Eng Struct Dyn 25:371–400

Atkinson GM, Boore DM (2003) Empirical ground-motion relations for subduction-zone earthquakes and their application to Cascadia and other regions. Bull Seismol Soc Am 93:1703–1729

Atkinson GM, Boore DM (2006) Earthquake ground-motion prediction equations for Eastern North America. Bull Seismol Soc Am 96:2181–2205

Beyer K, Bommer JJ (2006) Relationships between median values and between aleatory variabilities for different definitions of the horizontal component of motion. Bull Seismol Soc Am 96:1512–1522, Erratum (2007) 97, 1769

Bommer JJ, Abrahamson NA, Strasser FO, Pecker A, Bard PY, Cotton F, Fäh D, Sabetta F, Scherbaum F, Studer J (2004) The challenge of defining upper bounds on earthquake ground motions. Seism Res Letts 75:82–95

Bommer JJ, Scherbaum F, Bungum H, Cotton F, Sabetta F, Abrahamson NA (2005) On the use of logic trees for ground-motion prediction equations in seismic hazard analysis. Bull Seismol Soc Am 95:377–389

Bonilla MG, Mark RK, Lienkaemper JJ (1984) Statistical relations among earthquake magnitude, surface rupture length, surface rupture displacement. Bull Seismol Soc Am 74:2379–2411

Boore DM, Joyner WB, Fumal TE (1997) Equations for estimating horizontal response spectra and peak acceleration from western North American earthquakes: a summary of recent work. Seismol Res Lett 68:128–153

Campbell K (2005) Overview of Seismic hazard Approaches with Emphasis on the Management of Uncertainties. "2nd ICTP Workshop on Earthquake Engineering for Nuclear Facilities: Uncertainties in Seismic Hazard", Trieste, Italy 14–25 February 2005

Cramer H (1961) Mathematical methods of statistics, 2nd edn. Princeton University Press, Princeton

Deif A, Nofal H, Abou Elenean K (2009) Extended deterministic seismic hazard assessment for the Aswan High Dam, Egypt, with emphasis on associated uncertainty. J Geophys Eng 6:250–263

El-Hussain I, Deif A, Al-Jabri K, Toksoz N, El-Hady S, Al-Hashmi S, Al-Toubi K, Al-Shijbi Y, Al-saifi M, Kuleli S (2012) Probabilistic seismic hazard maps for Sultanate of Oman. Natural Hazard 64:173–210

Hanks TC, Bakun WH (2002) A bilinear source-scaling model for M-log A observations of continental earthquakes. Bull Seismol Soc Am 92:1841–1846

Hessami K, Jamali F, Tabassi H (2003) Major active faults in Iran. Ministry of Science, Research and Technology, International Institute of Earthquake Engineering and Seismol. (IIEES), 1:250000 scale map.

Johnson PR (1998) Tectonic map of Saudi Arabia and adjacent areas. Deputy Ministry for Mineral Resources, USGS TR-98-3, Saudi Arabia.

Joyner WB, Boore DM (1981) Peak horizontal acceleration and velocity from strong motion records including records from the 1979 Imperial Valley, California earthquake. Bull Seismol Soc Am 71:2011–2038

Kijko A (2004) Estimation of the maximum earthquake magnitude, Mmax. Pure and Appl Geophys 161:1655–1681

Kusky T, Robinson C, El-Baz F (2005) Tertiary–Quaternary faulting and uplift in the northern Oman Hajar Mountains. J Geol Soc 162:871–888

Reiter L (1991) Earthquake hazard analysis. Columbia University Press, New York, 254 p

Scherbaum F, Schmedes J, Cotton F (2004) On the conversion of source to site distance measure. Bull Seismol Soc Am 94:1053–1069

Slemmon DB (1977) State of the art for assessing earthquake hazard in the United States, Report 6; faults and earthquake magnitude: U.S. Army Corps of Engineers, Waterways Experiment Station, Vicksburg, Mississippi, Miscellaneous Paper S-73-1, 129 p.

Slemmon DB (1982) Determination of design earthquake magnitude for microzonation. Third International Earthquake Microzonation Conference proceedings 1:119–130

Stafford PJ, Strasser FO, Bommer JJ (2008) An evaluation of the applicability of the NGA models to ground-motion prediction in the Euro Mediterranean region. Bull Earthq Eng 6:149–177

Stepp JC, Wong I, Whitney J, Quittemeyer R, Abrahamson N, Toro G, Youngs R, Coppersmith K, Savy J, Sullivan T, Yucca Mountain

PSHA Project Members (2001) Probabilistic seismic hazard analyses for ground motions and fault displacements at Yucca Mountain. Nevada Earthqu Spectra 17:113–151

Thenhaus PC, Campbell KW (2003) Seismic hazard analysis. In: Chen WF, Scawthorn C (eds) Earthquake engineering handbook, chap. 8. CRC, Boca Raton, FL, p 50 p

Wells DL, Coppersmith KJ (1994) New empirical relationships among magnitude, rupture length, rupture width, rupture area, and surface displacement. Bull Seismol Soc Am 84:974–1002

Youngs RR, Chiou SJ, Silva WJ, Humphrey JR (1997) Strong ground motion attenuation relationships for subduction zone earthquakes. Seismol Res Lett 68:58–73